Chapter 2
Measurement, Tower, and Site Design Considerations

J. William Munger, Henry W. Loescher, and Hongyan Luo

2.1 Introduction

Although the number of sites making eddy-covariance (EC) CO_2 flux measurements throughout the world has increased rapidly over the last two decades it is still a challenge to define and build a new system. There are myriad options for tower design and placement and a steadily growing range of instrument options and configurations. Selecting among these options is based on finding an optimal solution that best achieves the precision and accuracy required to satisfy the scientific objectives for a site and often for the lowest installation and operational costs. Site design is only the first step to ensuring accuracy and precision of the results. Site operation must also include a program of quality assurance tests that verify whether the measurement system *as installed* is operating within the accuracy and precision goals over time. This calibration and validation is essential in knowing its overall performance, associated uncertainties, and for confidence in comparing data among different sites and within the same site over the duration of its operation. In this chapter, we provide theoretical basis and practical guidance for tower location and design and advice on instrument selection, installation, and operation.

J.W. Munger (✉)
School of Engineering and Applied Sciences, and Department of Earth and Planetary Sciences, Harvard University, Cambridge, MA, USA

H.W. Loescher • H. Luo
National Ecological Observatory Network, Boulder, CO 80301, USA

Institute of Alpine and Arctic Research (INSTAAR), University of Colorado, Boulder, CO 80303, USA
e-mail: hloescher@neoninc.org; hluo@neoninc.org

M. Aubinet et al. (eds.), *Eddy Covariance: A Practical Guide to Measurement and Data Analysis*, Springer Atmospheric Sciences, DOI 10.1007/978-94-007-2351-1_2,

2.2 Tower Considerations

One of the most important decisions is where to put a tower and the tower design and measurement locations. Inevitably there will be compromises between science requirements, engineering standards, cost and practicality. Although there is no ideal tower design or location, we point here to some guidelines based on theory and practice, and collected wisdom from the micrometeorology/biometeorological/surface-layer research communities. Installing a new tower site becomes a task of how to best minimize the systematic biases caused by a large suite of potential flow distortions and maintain the ecologic integrity of the site. Here we describe the source of these biases and present guidelines to optimize the scientific integrity of a research program employing tower-based measurements of eddy covariance (turbulent and gradient approaches) and micrometeorology. Understanding how the presence of tower and tower design affect the surrounding flows (wind) and microclimate, and identifying the issues to optimize the tower size, height, placement, physical properties, and orientation in order to minimize these effects are also the subject of this chapter section.

2.2.1 Theoretical Considerations for Tower Design

2.2.1.1 Diverse Ecosystems and Environments

Measuring an ecosystem microclimate and scalar exchanges above the canopy presents a unique suite of challenges. Ecosystems around the globe are structurally and functionally diverse as well as they are found in all the environmental extremes. Towers need to be designed to best capture the ecological drivers and processes from complex forest ecosystems to relatively simple grasslands. Towers, supporting infrastructure and instrumentation, have to be robust enough to withstand the expected environmental extremes over their lifetimes. In addition, the tower needs to provide year-round, safe access to instrumentation by technicians in extreme conditions, such as high temperatures, 0–100% relative humidity (RH), ice and snow loading, high winds, lightning, and nesting birds and insects; all of which provide unique design challenges.

2.2.1.2 Physical Effects on Surrounding Flows Due to the Presence of Tower Structure

The need to both make measurements through a plant canopy and to access the well-mixed surface layer above canopy presents the challenging requirement for a stable nonmoving platform that is inside a flexible and moving plant canopy. Though this is most physically challenging for measurements over forest canopies, short stature crops and grasslands are not free from these issues. Several types of distortion

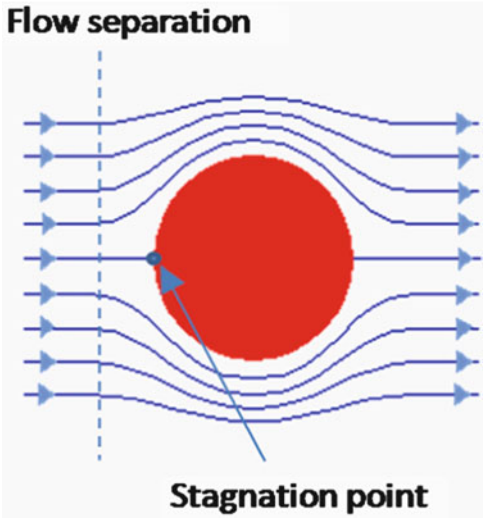

Fig. 2.1 Conceptual diagram of flow streamlines around an obstacle as viewed perpendicular to the flow (i.e., from the top of a vertical post). The point upstream where streamlines start to diverge is indicated by a *dashed line*. The stagnation point where flow velocity reaches zero is indicated by a *dot*

(streamline, wake, and chimney effects, etc.) can affect tower-based measurements. Each of these has to be evaluated for specific ecosystem types (structure and the environmental conditions) that a tower is to be placed into.

Wind Streamline Flow Distortion on the Windward Side of the Tower

The tower structure presents an obstacle to airflow and distorts the wind velocity and direction nearby. A schematic view of flow around an obstacle (Fig. 2.1) shows how the streamlines separate upstream of the obstacle. A stagnation point (windspeed = 0) forms in the upwind side of the obstacle due to the increased pressure field by the wind striking the obstacle. The flow is distorted for some distance downstream of the obstacle as well. Note the upstream distance affected by flow distortion increases with the size of the obstacle (Akabayashi et al. 1986). Wind speed decreases were observed at a distance of 1 tower diameter in front of and on the windward side of the tower at a constant 9.2 m s^{-1} wind speed inside a wind tunnel (Cermak and Horn 1968). In the windward side of an ocean-deployed tower platform, wind speed was decelerated by up to 30% within 1 tower diameter away from the tower (Thornthwaite et al. 1962, 1965). Recirculation flows were also observed within the region of separation downstream (Davies and Miller 1982) (Fig. 2.2).

Wind Flow Distortion on the Lee Side of the Tower

Wind speeds are attenuated on the lee side of a tower, that is, the wake area. Moses and Daubek (1961) reported up to 50% decrease in wind speed for light winds and a

Fig. 2.2 View from the side of the obstacle. Conceptual diagram for windward flow distortion and lee-side flow distortion

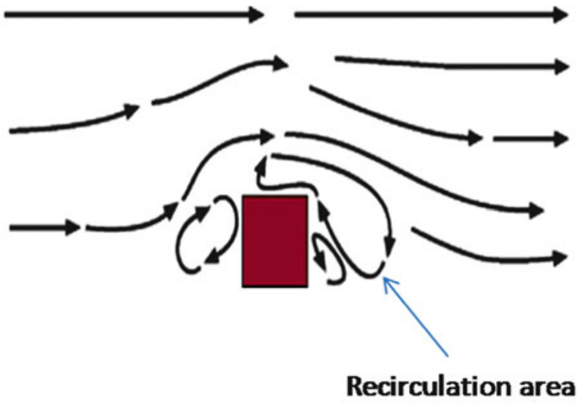

decrease of 25% at 4–6 m s^{-1} in the wake area from a 2 m × 2 m cross section tower. Similarly, wind speed decreased by 7% for 8–12 m s^{-1} in another report (Shinohara 1958). Wake effects behind an obstacle apparently reduce in size and magnitude as wind speed increased because of more rapid restructuring of turbulent flow. In a wind tunnel experiment, a decrease of 40% at a distance within 2 tower diameters at a 9.2 m s^{-1} wind speed was also observed (Cermak and Horn 1968) (Fig. 2.3). This wake effect occurred in a well-defined, constrained ±30° sector from centerline, downwind. The wake effects are affected by the size (both length and width) of the obstacle.

Wind Flow Distortion on the Sides of the Tower

As air flows around a tower, the tower changes the flow streamline, and results in the acceleration of wind around the sides of tower. This acceleration is due to decreased pressure on both tower sides and act as a jet (Munson et al. 1998). The maximum accelerated wind speed within both jets was 18% on an in situ "boxlike" platform (Thornthwaite et al. 1962, 1965). Moreover, the increase in flow along the tower sides, up to 19%, was observed in another experiment (Dabberdt 1968). In a wind tunnel experiment, flow around the tower sides was increased up to 6% at distance between 1 and 2 obstacle diameters (Cermak and Horn 1968).

Wind Flow Distortion at the Top of the Tower and Chimney Effects

When air flow passes a vertical obstacle (tower in our case), it separates and accelerates around the obstacle sides and top. The separated flows also accelerate vertically along the wall of the obstacle (Fig. 2.4). The upward deflection and acceleration of winds in the windward side of a tower were observed (Fig. 2.5, Sanuki and Tsuda 1957). Wind speed acceleration at the upwind leading edge of a boxlike platform was observed up to 40% (Thornthwaite et al. 1962, 1965).

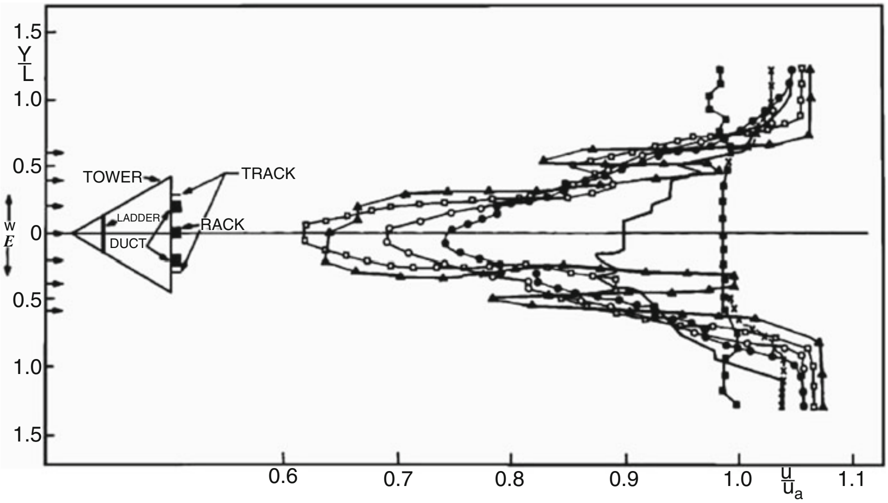

Fig. 2.3 Transverse velocity profiles, tower model, showing lateral variation across the wake for several downstream positions made in a wind tunnel. Additional Note for Figure 2.3: Units for the axis are normalized according to engineering nondimensional analyses, where the *y*-axis is the measured crosswind component (v) and normalized by the physical length scale (L), and the *x*-axis is the measured longitudinal wind speed (u) and normalized by the constant, controlled wind speed in the tunnel (u_a), where u_a was 9.2 m s^{-1} and mounting was at 0°. *Solid square*, station −1 (−37.5 cm); *cross*, station 0, (0.00 cm); *solid triangle*, station 1 (37.5 cm); *open square*, station 2 (75 cm); *open circle*, station 3 (150 cm); *solid circles*, station 4 (300 cm); *solid line*, station 5 (750 cm) (Reproduced from Cermak and Horn (1968))

Fig. 2.4 View from the side of the obstacle. Conceptual diagram to show the vertical deflection of airflows (chimney effects)

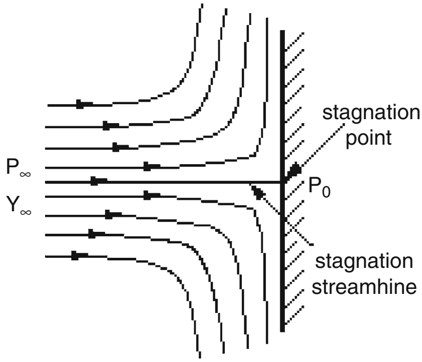

Heating of the tower base and strucuture induces convective circulation that may reinforce the vertical deflection, leading to a strong ‘chimney’ effect that preferentially move air from the near the ground up to the top of tower. This type of effect is a function of how much tower (and foundation) mass is present, its spatial distribution, heat capacity of the tower and foundation, structural shape of the tower,

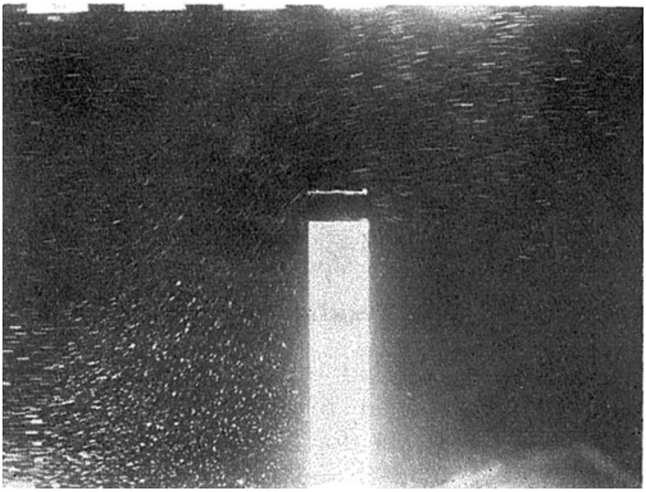

Fig. 2.5 Flow around an anemometer tower with a roof at a height equal to a tower diameter. Upward deflection and acceleration of winds were observed in the windward side of a tower (Sanuki and Tsuda 1957)

degree of disturbance to the existing plant canopy (openings or clearings made in the ecosystem during tower construction), and the amount of input net radiation to the ecosystem. Any factor in site design or implementing tower-based measurements that alter the natural conditions enhances these effects.

Site disturbance can alter the localized convection around the tower by removing plant material, leaf litter, and disturbing the soil. If the ground heats up more (or foundation for that matter) than prior to site disturbance, the amount of net radiation and albedo will change, generating local circulations around the tower. Similarly, large tower structure, large tower foundations, increased concrete mass, and increased disturbance will all generate additional convection and enforce chimney effects. Concrete foundations of the tower as well as the metal structure heat up faster due to their lower heat storage capacity than the surrounding soils. To reduce this effect, wherever possible, smaller tower structure and smaller concrete foundation are preferred for the tower establishment.

2.2.1.3 Size of Horizontal Supporting Boom

At the 1976 International Turbulence Comparison Experiment, some participants reported mean upflow wind speed of $0.1\ \mathrm{m\,s^{-1}}$ caused by the 0.05 m diameter horizontal support structure (Dyer 1981), which was large enough to invalidate eddy covariance measurements. Therefore, the size of the mounting boom for anemometer also needs to be minimized, and should only be sized to provide a secure and stable measurement platform.

2.2.1.4 Tower Deflection and Oscillations

The physical stability of the tower can affect the measurement of winds and turbulent structure (Barthlott and Fiedler 2003). Because the eddy covariance technique utilizes the covariance between wind speed and scalar concentrations, that is, turbulent fluctuations of temperature, CO_2, H_2O, etc., any movement in the tower that covaries with either the turbulent fluctuations of wind speed or scalar that is in interest, for example, towers that sway with the wind, or wind-induced harmonic motion or vibrations, contributes toward uncertainty in the estimates. The current ability to measure wind speed accurately is 0.02 m s^{-1}, consequently, tower or boom movement are required to be below this threshold and shall not have moments that covary with the wind between 1 and 20 Hz (harmonic effect). Fast response accelerometers can be used to quantify this motion. Movement due to personnel working on the tower can be discounted, because the movement they generate does not covary with wind or scalar exchange and data recording may be suspended anyway while personnel are on the tower servicing instruments. It should also be noted that tower sway makes it uncomfortable for personnel to work on the tower structure.

2.2.1.5 Recirculation Zone at the Opening in a Tall Canopy

After flow passes an obstacle, wake effects due to the pressure gradient form a recirculating flow (Arya 1988) (Fig. 2.2). This flow can be caused by canopy edges (Chen et al. 1990, 1992, 1993a, b), by the creation of openings in the canopy for tower access, or by other structures such as buildings (Fig. 2.6, note the return flow pointed by the lower wind vane, which is opposite to the top wind vane, (Vaucher et al. 2004)). Recirculation areas form in canopy openings with a horizontal length scale (distance) equal to 2–5 canopy heights (i.e., the vertical length scale, Fig. 2.7, Detto et al. 2008). The size of the recirculation area can vary from 1 to 15 canopy heights, depending on the width to height and length to width ratios of the contributing obstacles (Arya 1988). This is still a concern even in nonforest ecosystems, though the affected areas are smaller and the sensors are closer to the ground. The larger the obstacle (tower) size, the larger the tendency to have larger recirculation areas. The returning flow also increases the propensity of up-flows and reinforces the chimney effects, which could significantly bias wind measurements as well as perturb mixing ratio gradients. To avoid the man-made formation of recirculation areas, the size of the openings in canopy should be minimized during the construction and tower placements. Also, the removal of trees and branches, which provide resistance (drag) against the formation of these recirculation areas, should be minimized. Flow recirculation is most obvious in tall stature, forest canopies, but it must still be considered even for short grass and crop canopies. Note that in a short canopy, the scales of support structures and sensors will be larger relative to the canopy height.

Fig. 2.6 An experiment to show the cavity flow with westerly flow (10 m above ground) over the top of a building and easterly return flow at 2 m above ground (Reproduced from Vaucher et al. (2004))

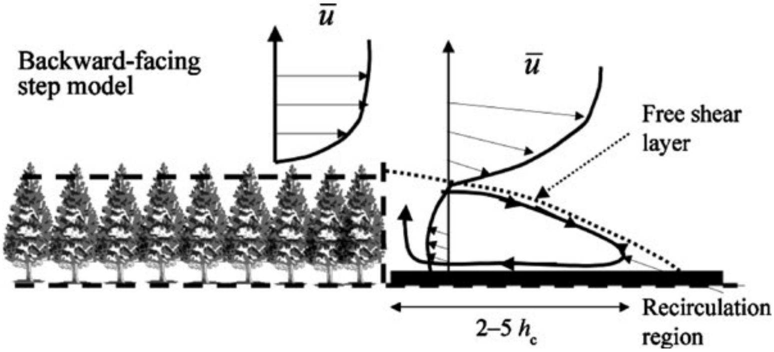

Fig. 2.7 Conceptual model for the structure of turbulence near forest edge (Detto et al. 2008). Recirculation areas form in forest openings with a length (distance) equal to 2–5 canopy height (h_c)

2.2.2 Tower Design and Science Requirements

2.2.2.1 Tower Location Requirements

The tower should be located in a representative ecosystem of interest. Micrometeorological requirements include adequate fetch for all desired wind directions and atmospheric stabilities, and should be centered in or on the downwind side of a spatially homogeneous and structurally uniform vegetative canopy, which in practice is often difficult to achieve. The tower (and associated boom orientation) should also be positioned to maximize the exposure time for winds blowing from the desired land cover type, and with the longest upwind fetch attainable. Because some ecosystems do not have a uniform cover type, the prevailing winds, land cover type, and topography should be analyzed to determine the source area under different stabilities, wind speeds, and direction, and will provide valuable guidance for appropriate tower placement (see Chap. 8 and Foken and Leclerc 2004; Horst 2001; Horst and Weil 1992, 1994, 1995; Kormann and Meixner 2001; Schmid 1994; Schmid and Lloyd 1999; Schuepp et al. 1990). In complex terrain, placement of the tower should be situated to minimize flows toward or away from the site and to minimize horizontal flux divergence, advective motions, and drainage in the airshed (Lee 1998; Loescher et al. 2006a; Paw et al. 2000).

Discontinuities in ecosystem structure, which can also affect local circulations, flows, and subsequent measurements, should be avoided in tower site selection. Plant canopies are dynamic and can also alter the structure and increase surface heating through natural disturbance even after a tower has been erected, for example, tree falls, windthrow, and manmade disturbances, for example, logging, harvests, clearings, roads, development, and even the gap created to allow a tower to pass through a plant canopy. Even in micrometeorologically ideal locations (uniform source/sink strength, flat and even terrain, plant canopy, and short roughness lengths), studies have demonstrated that small clear-cuts changed the local circulations during periods of convective turbulence and changed the flow statistics at a tower site (Leclerc et al. 2003; Loescher et al. 2006a). Anomalous flows can also occur and affect tower-based measurements even in short-stature vegetation when the surface conditions are modified from the desired conditions (e.g., homogeneous-managed conditions perturbed by harvest, grazing, mowing, etc.). Even these seemingly small, microscale discontinuities in stature and conditions can perturb wind fields and patterns of latent and sensible heat, or be unrepresentative of the local microclimate, for example, temperatures, long- and short-wave radiation, reflected photosynthetically active radiation (PAR), etc. In another example, low-level jets can descend through the boundary-layer and can alter flows around a tower (Karipot et al. 2008, 2009). These flows, however, are temporally uncommon and can easily be removed from datasets once they are identified. Standing waves can be quite common, and occur with conditions of mechanical turbulence, high wind speeds, and over short stature ecosystems with undulating topography, such as dunes, grass fields, prairie, and tundra. These anomalous flows can cause directional systematic bias in datasets. Even after a site has been chosen and tower has been established, datasets should be examined with rigor periodically. Relocation of tower should be considered if these flows are detected.

Criteria to site a tower are also contingent on the scientific requirements for the research study or program in interest. Minimizing the flows induced by the tower infrastructure toward or away from a site becomes important in reducing uncertainties in EC and local-scale micrometeorological estimates at the seasonal-to-interannual time scales rather than process-based studies. This is because the relative magnitude of uncertainties can change diurnally or alter with synoptic-scale changes in climate.

While there are no uniformly accepted criteria, a general guideline to site a tower is to have adequate fetch to measure the representative ecosystem in question among the expected environmental conditions, that is, $\geq$80% contribution by the representative ecosystem with the design goal of 90% contribution. Annual and interannual net ecosystem exchange (NEE) estimates benefit from contiguous time series over as much of the source area as possible making the $\geq$80% contribution of the source area to these measurements paramount. Whereas process-based studies or campaign-based studies can constrain measurements to a predefined suite of environmental conditions, for example, select time period, summer light response curves in unstable atmospheres, or nighttime NEE with $u* > 0.25\ \mathrm{m\,s^{-1}}$, and limit the number of averaging periods only during times when the $\geq$80% criteria is met. Estimating uncertainties during the postprocessing of eddy-covariance data can also be used as a robust diagnostic tool to assess proper tower location (Göckede et al. 2004, 2006, 2008), where footprint and directional analyses, topography, and vegetative mapping can be used in concert to diagnose data quality.

Other ecological criteria may also be important when considering the location of the tower, such as avoidance of wildlife migrations path (e.g., corridor of seasonal caribou movement), or breeding grounds for endangered species. All final decision-making and criteria for specific tower site locations should be documented, archived, linked to best available practice, and attached as metadata to the datasets collected from the tower.

2.2.2.2 Tower Structure Requirements

Most available commercial towers are commonly made of steel or aluminum. Safety and access issues and the need to comply with appropriate regulations and design criteria are not discussed here. Local tower erection companies should be consulted. The material itself, however, is less important than its ability to meet site-specific science requirements, which does include some tradeoffs between size and stability, and flow-distortions and thermally induced chimney effects. Tower with a large projected footprint ($>6\ \mathrm{m^{-2}}$) may be very stable and appropriate for large forest structure, but inappropriate for short-stature forested canopies with high stem density. The structural integrity of the tower should have minimum sway, harmonic motion, or vibrations. The tower movement should be <1.0 mm per 1 m in height when subjected to personnel on the tower or with windspeeds equal to of less than $20\ \mathrm{m\,s^{-1}}$. The tower should not oscillate within the 1–20 Hz frequency. It is not uncommon for towers to fail to operate correctly once weight loading by instruments, ice, and personnel exceeds the structural requirements. Towers must also be capable of supporting measurements made within the range of expected environmental conditions, for example, winds to $40\ \mathrm{m\,s^{-1}}$, humidity ranging 0–100%, temperature range of -50°C to $+50$°C, salt air, ice (12.7 mm of accumulated ice), snow (weight, 5.1 m year^{-1} in depth), and rain (0–6.35 m year^{-1}). Hence, safety issues aside, a tower system should be site specifically designed to have sufficient strength and stability to simultaneously withstand the weight loading, applied temperature and/or other accompanying environmental phenomena without experiencing yielding, failure, or detrimental deformation. More specific guidelines and requirements may be mandated by local zoning and permitting procedures, which must be followed. Tower size should be optimized to meet safety and regulatory requirements while also supporting the necessary instrumentation. Excessive tower size increases the local impact on the nearby environment by perturbing the local microclimate and inducing flow distortions noted above.

Tower design and materials should attempt to minimize the thermal mass and reflective surfaces that can alter the radiation environment, that is, short wave, long wave, ultraviolet, infrared, albedo, and temperature spectra. Reducing the exposed thermal mass and minimizing changes to the radiation environment will reduce the propensity of localized tower-induced convection and chimney effects. The tower structure should also not create safe harbor for stinging insects or dangerous animals, for example, snakes, scorpions, raccoons, bears, and hunters. Fences climbing prevention hardware, and appropriate warning signs are generally needed to prevent unauthorized human access.

2.2.2.3 Tower Height Requirements

Towers must have the ability to access the environment through and above the plant canopy. The tower shall be high enough to place the sensors at top layer well above the surrounding plant canopy in the well-mixed surface layer, but not so high that the footprint during stable night-time conditions extends beyond the boundary layer above the ecosystem of interest. Nor shall the tower height be too low such that the tower top measurements are influenced by the roughness layer or individual canopies close to the tower.

Because of the wide range of structural and functional diversity of ecosystems, two separate criteria will be applied to determine the tower height for the top measurement level: (1) a fixed tower-measurement height (h_m) of 6 m above all grasslands (or shrublands) where $h_m > [d + 4(h_c - d)]$ and $h_c \leq 1.75$ m, h_c is the mean canopy height and d is the zero plane displacement height (Monteith and Unsworth 2008), and (2) $h_m \approx d + 4(h_c - d)$ over forested or more structurally complex ecosystems. Both criteria are founded on the work from multiple studies (e.g. Dyer and Hicks 1970; Hicks 1976; Lemon 1960; Monin and Obukhov 1954). If a research program has many towers among several ecosystem types, the criteria used should maintain consistency and uniformity among tower measurement heights within any particular ecosystem type to provide regional and spatial comparable data with similar uncertainties.

There will be some instances when the canopy height will change over time (e.g., actively growing young forests and crops). In these cases, the tower design needs to incorporate the capability of changing tower height and moving sensors over time. Eddy covariance measurements should be maintained in the same turbulent structure at $d + 4\ (h_c - d)$ to maintain the same relationship with ecosystem structure for any gradient measurements, and maintain the same source area for any downward facing sensors. For sites that are actively accruing canopy height, plan to construct the tower at least 5 $(h_c - d)$, but mount the sensors at $d + 4(h_c - d)$ at inception. The tower and measurement height shall be changed at a convenient time of the year when the height of the sensors (h_m) is $< d + 3.6(h_c - d)$. For crops with changing canopy heights that remain below 3 m, 8 m is the suggested measurement height. Horizontal wind profiles measured at the tower sites can be used to determine d.

2.2.2.4 Tower Size Requirements

Tower size (horizontal dimensions, not height) shall be large enough to be safe and secure for many years of operation, but should also limit the impact on the surrounding environment and scientific measurements of interest and minimize the flow distortion as described earlier in Sect. 2.2.1.2.

Large tower structures create larger canopy openings, which promote wind recirculation (see Fig. 2.7), enforcing chimney effect, changing the local microclimate, and, for the biological concerns, introducing opportunistic plant species, which will locally alter ecosystem structure around tower due to the radiation and temperature changes at the opening (edge effects). Minimizing the tower foundation and canopy opening shall be implemented to limit disturbance and to mimic the natural environment. For the same reason, adjacent vegetation shall not be removed or disturbed unless absolutely necessary.

There are site-specific interactions between the tower presence, ecosystem type and structure, and local microclimate. As a general guideline for tower design and establishment, the spacing between tower and nearby trees should mimic the existing mean distance between trees (i.e., mimicking the existing natural ecosystem structures and openings).

In order to minimize tower-based uncertainties, a custom-tailored tower design to site-specific environmental conditions is ideal, but not practical. To reduce the uncertainties of tower effects on the same suite of measurements made among multiple tower sites within a certain research program, the projected tower base is recommended to be no larger than 4 m^2, for example, 2 m $\times$ 2 m, because (1) sources of uncertainty caused by the tower design among all sites will be similar and (2) this will enhance the interchangeability of all sensors and supporting hardware, and uniform tower health and safety training. Special consideration can be made to increase the tower structural members (and size of the projected base) for closed plant canopies if the average projected tree crown area is $>6\times$ the tower projected area (4 m^2), that is, >24 m^2, canopy cranes. On the other hand, at nonforested sites, structural elements should be minimized because there is no canopy to mask the tower.

Tower shape also has some bearing on the ability to meet site-specific criteria and scientific requirements. Some researchers prefer triangular climb-up towers (antennae-style) because they are light weight and can be easily transported into remote areas, small foundations are needed, small holes through the plant canopy can be created, and minimal impact on the surrounding microclimate can be achieved. They do, however, have limited expansion room for additional science and instrumentation. It is important to properly account for the weight and especially surface area of instrumentation on the tower to not exceed the design specifications. Furthermore, since the tower structure serves as the climbing structure, design and placement of instruments, booms, and cables needs to be considered to avoid interfering with safe tower access. Walk-up scaffolding-style towers are larger with likely more flow distortions, create large canopy access holes, and require larger foundations. They do, however, allow simpler instrument-mounting options without interfering with tower access (up to the limits imposed by not having sensors interfere with one another), and personnel may be more comfortable using stairs rather than ladder-style climbing. In either case, appropriate fall-restraint systems are necessary. Selecting a tower style is partly a matter of taste and optimization of construction and operation costs against scientific returns, and matching the tower design to the specifics of local ecosystem structure. The considerations noted above provide guidance on measurement issues to be considered.

2.2.2.5 Instrument Orientation Requirements

The tower, instrument placement, and overall design should minimize any disturbance to the radiation and other microclimatic environment of interest (Culf et al. 1995, 1996). Challenges to measure the surface layer (and microclimate within a plant canopy, Sect. 2.5) occur when, by necessity, the tower and supporting structure have to be fixed, stable, and surrounded by a flexible plant canopy. The tower and booms that extend horizontally out from the tower superstructure have to be positioned within, close to, and able to assess the ecological strata of interest (ecosystem structure, microclimate, etc.). This will be partially dependent on minimizing the gap size in the plant canopy created by the tower. All the meteorological measurements (with the exception of radiation) should be mounted on a stable horizontal boom with a minimum distance that is no less than the length of 2x the face-width of the tower. Anemometers should not be mounted on the tower sides, or in the wind wake area, and should be placed on the windward side of tower on a stable horizontal boom. Gill et al. (1967) suggested that, to achieve wind speed measurements, accurate to within 5%, anemometers should located no less than 2 tower diameters from an open lattice cylindrical obstacle. This finding can also be applied to the face-width of square, rectangular, or triangular towers. The windward side is the one facing the site-specific predominant wind direction, which is where booms should be mounted for EC measurements. However, for sites with distinct differences between daytime and nighttime wind directions, the preferred orientation for anemometers should be optimized to measure the daytime winds. Wind measurements made when the anemometer is not facing the streamline need to be inspected for biases and distortions. If anemometers are mounted directly above the tower top (not recommended), they must be mounted at least 5 tower diameters above the tower top (Perrin et al. 2007).

2.2.2.6 Tower Installation and Site Impact Requirements

During tower construction, installation, and operation, extreme care shall be given to minimize any impacts on the surrounding environment in order to minimize perturbations to the ecological variables that we wish to measure, for example, small canopy openings, reduced thermal mass of tower structure and foundation, boardwalks not in the view shed of sensors, etc. Extensive clearing around the base of the tower or use of large construction equipment should not be permitted. Boardwalks should be considered if impact to the surround soil and plants is expected to increase seasonally and over time.

Although the tower structure can be robust, special consideration is needed to address site-specific conditions, for example, sites with marine salts or areas with sand storms may need more frequent painting and protection from rusting. Higher winds in alpine environments may require a stronger, well-guyed tower to maintain the stability requirements, while other sites may not allow guy wires because they interfere with migrating birds. Regularly scheduled tower inspection and preventative maintenance according to tower manufacturer recommendations are essential for assuring site reliability and safety of personnel. Guy wires may be applied wherever permitted to secure tower stability and to withstand high winds, though guy wires can become a source of tower failure in tall-stature ecosystems if trees or branches frequently fall and are massive enough to break a guy. Cross hatched guys, or cross braced, and free of any contact with trees or branches are recommended to ensure that the tower is stable and safe.

In many locations lightning is common and measures need to be taken to minimize the potential for instrument damage and loss of data. Proper grounding of the tower, guy wires, anchors, and buildings is an essential component of construction. Induced voltages could occur in long signal wires from sensors to data acquisition systems. It is inexpensive insurance to place surge voltage protectors (varistors, suppression diodes, gas-discharge tubes) or optical isolators on each signal or control line, including serial and network communications. An excellent connection to earth ground is essential for diverting surges and avoiding buildup of stray voltages. Obviously, site personnel should never risk their lives by working on or around a tower when lightning storms are nearby.

Many towers require a shelter near the base of the tower to house instrumentation, gas cylinders, and supporting equipment. Its structure and placement should not affect the local biotic and abiotic environment of interest. Placement of the shelter can be adjacent to the tower if there are closed-canopy conditions which can shield the tower measurements from changes in microclimate caused by the shelter, for example, reflected radiation, changes in turbulent structure, heat, traffic, etc. Otherwise the shelter should be located away from the tower. In order to rigorously minimize impacts of the shelter on measurements, the location of the instrument shelter shall be on the prevailing leeward side of the tower (site specific). The distance between the tower structure and the instrument shelter shall apply a 5:1 ratio of tower-shelter horizontal separation to shelter height (optimum for grasslands) or 3:1 ratio (minimum for closed forest canopies). Exterior color should mimic the color and environmental reflectivity (albedo) of the surrounding landscape, and the roof design, type, and slope should minimize perturbations to air flows affecting the tower measurements.

2.3 Sonic Anemometer

2.3.1 General Principles

Eddy covariance flux measurements are based on determining the correlation between changes in vertical wind velocity and deviations in a scalar quantity such as mixing ratio of a trace gas or air temperature (see Chap. 1). The measurements must be frequent enough to capture the variability due to atmospheric turbulence, which is typically >1–10 Hz depending on the surface characteristics as discussed in Chap. 4. The principle of sonic anemometry-thermometry (SAT) was demonstrated prior to the 1960s (Kaimal and Businger 1963a, b), and was developed into more robust field deployable instruments in the 1970s (Campbell and Unsworth 1979). Availability of reliable and relatively inexpensive three-dimensional SAT was a key technology allowing the extensive networks of CO_2 flux measurements that exist today. The basic principle of a SAT is to measure the difference in transit time for an ultrasound pulse between pairs of transducers arranged at a known distance apart (d_{pl}). Transit time (t) is dependent on the speed of sound and velocity of air in its path, hence the difference in the inverse of transit times for sound pulses traveling in opposite directions along the same path depends on the wind velocity (u_{pl}) along the transducer axis and the speed of sound (c) can be derived from the sum of the inverse of transit times:

$$u_{pl} = \frac{d_{pl}}{2}\left(\frac{1}{t_{1,2}} - \frac{1}{t_{2,1}}\right) \tag{2.1}$$

$$c = \frac{d_{pl}}{2}\left(\frac{1}{t_{1,2}} + \frac{1}{t_{2,1}}\right) \tag{2.2}$$

where d_{pl} is the path length and $t_{1,2}$ and $t_{2,1}$ are the transit times from transducer 1 to 2 and 2 to 1, respectively.

Speed of sound is a function of air density, which depends on temperature and the mixing ratio of other gases, especially water vapor. The equations relating speed of sound to temperature are presented in Sect. 3.2.1.1.

2.3.2 Problems and Corrections

Although SAT measurements are grounded in physical principles, several critical issues affect the measurement when applied to field practice. Nearly all these issues are dealt with in the SAT software by theory-based and empirical correction terms. In most cases, users don't need to consider them explicitly, but should be sufficiently aware of these underlying issues to recognize when results might not be valid. The fundamental data measured by SAT is the delay time for a sonic pulse. However, there is finite delay between applying an excitation voltage to a transducer and generation of a sonic pulse. The delay is affected by the transducer temperature and must be accounted for by factory calibration and built-in corrections.

The path that a sonic pulse takes between a pair of transducers is distorted by winds oriented across its axis, giving rise to crosswind contamination of sonic temperature measurements. They must thus be corrected for this effect. Current sonic anemometers include this correction in their firmware, but this is not the case for the older Solent R2 models and the METEK USA1 without a turbulence processor. The correction was first given for anemometers with Cartesian coordinate systems (Schotanus et al. 1983) and recalculated for the omnidirectional probes (Liu et al. 2001):

$$\left(\overline{\omega'\theta}\right)_{\text{corrected}} = \left(\overline{\omega'\theta}\right)_{\text{uncorrected}} + \frac{2\overline{\theta}}{c^2}\left(\overline{u}\,\overline{u'\omega'}A + \overline{v}\,\overline{v'\omega'}B\right) \tag{2.3}$$

The coefficients A and B are given in Table 2.1.

Finally, the supporting structure of the SAT can also perturb the flow by blocking portions of the measurement volume or generating small-scale turbulent eddies and wake effects, and as discussed above, the measurement platform itself (boom and tower) obstructs the wind (discussed below). The effects of flow distortion and shadowing by the transducers have been extensively analyzed, (Dyer 1981; Kaimal et al. 1990; Miller et al. 1999; Wyngaard 1981), and SAT manufacturers have incorporated these results into probe design, calibration, and data processing firmware. This point is discussed more in details in Sect. 4.1.5.1. Users don't need to make corrections but these considerations impose limits on the data range that is acceptable for the SAT they are using. In particular, the attack angle (deviation of the wind streamline from horizontal) should be considered and checked that it

Table 2.1 Coefficients for Eq. 2.3 according to Liu et al. (2001), φ: angle between the measuring axis and the horizontal line for different sonic anemometer types currently in use. For most of the recent sonic anemometers, the correction is included in the firmware (except older R2 and USA1 without turbulence processor)

Factor	CSAT3	USA-1	Solent (all other types)	Solent-R2
A	7/8	¾	1 − 1/2 cos2φ	½
B	7/8	¾	1 − 1/2 cos2φ	1

is within the range that the SAT specifications indicate as valid. Large errors can arise for winds outside that range (Gash and Dolman 2003). Early versions of three dimensional sonic anemometers used an array of transducers arranged on orthogonal axes to measure the three components of wind velocity to simplify construction and directly provide velocities in an orthogonal coordinate system. This turns out to not be an optimal geometry, in part because self-shadowing is large for winds aligned with one of the transducer axes. Most SAT now available employ nonorthogonal configurations. Trigonometric axis transformations are made in signal processing to derive the orthogonal components of each wind vector using results from all the transducer pairs collecting data from the same physical volume (Sect. 3.2.4). Improvements in the design and fabrication of ultrasonic transducers have made them smaller and more reliable.

2.3.3 Requirements for Sonic Choice, Positioning, and Use

Today, several manufacturers provide fast sonic anemometers suitable for flux measurements. Typically SATs cycle through the measurement axes more rapidly than the data reporting rate and the output data are the result of averaging several separate measurements for each axis to reduce noise. Signal processing algorithms can generate data quality flags to identify potential errors. Results from SAT intercomparisons in a controlled environment highlight some distinctions between them and point to key design attributes to consider in selecting an anemometer (Loescher et al. 2005). In general "yoke" style SAT, with transducers arrayed at the end of a horizontal boom, are preferable to "post" style units in which the transducers are arrayed above the support structure creating asymmetrical flow distortion. Deviations were observed even within the manufacturers specified acceptance angle. Even after accounting for the influence of water vapor on temperature inferred from SAT (see Sect. 3.2.1.1), it is not recommended as an accurate absolute temperature measurement, but it can be calibrated against a collocated reliable absolute temperature measurement to correct for any offset that could be imparted by uncertainty in the transducer delay time for instance. After calibration, the absolute temperature from SAT is suitable for inclusion in flux calculations such as computation of molar volume. In most cases, the temperature errors are a constant offset and do not impact the computed variances and covariances. Some models of SAT, however, exhibit a nonlinear dependence of sonic temperature on absolute air temperature so that the fluctuations in temperature ($\theta' = \theta - \overline{\theta}$) are neither symmetric about the mean nor constant as the magnitude of θ changes, resulting in incorrect temperature covariances, making them unreliable for heat-flux measurements. Transformation from buoyancy flux – which is what the SAT delivers – to sensible heat flux is described in Sect. 4.1.2.

SAT specifications are continually evolving, making it impractical to recommend a specific manufacturer and model as ideal. Instead, we provide a set of overall attributes to consider in selecting a new SAT. First of all, a 3-axis SAT is required to make eddy covariance measurements. Two-axis versions that are intended for measuring horizontal wind speed and direction only are not suitable. Measurement accuracy and precision is affected by the quality of the transducers electronics and calibration. Research grade SATs that are suitable for eddy covariance will use better transducers with minimal temperature sensitivity and better electronics components with improved accuracy to measure the very small differences in signal transit time at very low wind speeds. Research-grade SATs will typically have resolution of 0.01 $m\,s^{-1}$ and 0.01°C, or better, for wind and temperature, respectively, that are required to measure the respective turbulent fluctuations. SAT measurements are affected by local environmental conditions. Because transducer performance is affected by temperature, the data processing and internal calibration tables must account for this temperature dependence in the pulse transit times. Be sure to select a model that has an operating temperature that spans the expected local range, or select optional shifted range as appropriate. Raindrops and ice, which block the transducer path and attenuate the sound pulse, degrade SAT measurements. All SATs will fail in very heavy rain or under icing conditions when the sound pulses are attenuated too much. In light rain conditions (e.g., <0.5 mm h^{-1}), transducer geometry, selection of materials, wicking, and proprietary signal processing algorithms are solutions to minimize data loss. Angled transducer surfaces are less prone to accumulate water droplets that block sound transmission, which is an advantage for nonorthogonal versions compared to orthogonal heads where the transducer face of the vertical axis is horizontal. Additionally, hydrophobic materials and physical design of the transducer to wick droplets away improve performance or speed recovery after the end of rain event. Finally, SAT manufacturers have developed proprietary internal software to improve performance in the face of some signal degradation. In cold environments, optional heating elements to prevent icing on the transducers may be necessary. Measurement accuracy depends on knowing the path length between transducers. The sonic array must be handled with care to avoid bending the support arms, and returned for recalibration if any accident changes the alignment.

The mode of data output and power requirements are additional considerations; SAT data are typically generated in digital form and optionally available as analog output via some internal digital to analog conversion. Other analog signals can be optionally sent to the SAT and digitized by on-board electronics to be included in the SAT output stream providing a way to merge data from other sensors with the wind data. Data logging time stamping and clock maintenance options are discussed in more detail in Sect. 2.1.

Although the SAT provides wind speed and direction, an independent measurement of wind speed and direction is desirable for comparison and redundancy. The traditional wind vane and spinning cup anemometer is a typical approach for wind measurement. Alternative configurations use an integrated vane and propeller configuration. Two-axis sonic anemometers that are priced competitively with the best quality mechanical anemometers are available. All mechanical anemometers need a minimal wind speed (typically 0.1–0.2 ms^{-1}) to overcome inertia of the vane and the cup (or propeller). Minimizing the mass of the components and friction in the moving parts reduces the threshold, though it can increase fragility of the device. Optimizing this tradeoff depends on the range of wind speeds likely to be encountered at a site, and how dependent the science questions are to the accuracy of low wind speed measurements. Wind sensors need to be located upwind of supporting structures to minimize artifacts and errors due to flow distortion and wake effects. A single measurement at an arbitrary height above the canopy has limited value as a network measurement. Multiple measurements that observe the wind speed profile near the canopy interface can be analyzed to define drag coefficients, roughness lengths, and zero plane displacement height based on the assumption of logarithmic wind profile. In order to provide a cross-check on SAT measurements, it is essential to perform sensor maintenance according to manufacturer guidelines and monitor the data itself to check for changes in the low-speed threshold. Moving parts, such as bearings, will wear over time and must be replaced periodically to ensure consistent data.

Corroboration of sonic temperature would require a secondary measurement of ambient temperature. Precise and accurate temperature measurements are possible using any of the typical temperature-sensitive devices (thermistors, thermocouples, platinum resistance thermometers) as incorporated in commercially available temperature probes in conjunction with appropriate signal conditioning and data logger connections that will be described in sensor documentation. Proper shielding of the measurement sensor from solar heating and radiative cooling is essential for unbiased temperature measurements. Fan-aspirated radiation shields provide the most effective radiation shielding and will reduce heating errors to 0.1° or less, independent of wind speed and radiation intensity.

In addition to comparing horizontal wind and sonic temperature against independent wind and air temperature measurements, tracking the ratios of variance and means of the wind components helps to identify sudden changes in performance or wind sectors with anomalous data that should be investigated (Tropea et al. 2007). Some SATs include a "zeroing chamber" that can fit over the transducer array without interfering with the signals. This chamber is used to verify that none of the transducer pairs have a zero-offset when measuring in a zero-wind condition, and to adjust the internal constants if necessary. Data quality checks are discussed in more detail in Sect. 4.3.

The characteristics of sonic anemometers, as well as of gas analyzers (see below), and their location make them act as filters that remove high- and low-frequency components of atmospheric signals and reduce the magnitude of the measured flux. Several correction procedures to account for lost flux components are presented in Sect. 4.1.3. Here we discuss design considerations to minimize the magnitude of these corrections. Spatial averaging along the path length of the sonic anemometer or a gas analyzer and spatial averaging due to the separation between velocity and scalar sensors are important causes of low-pass filtering. Therefore, path length and separation should be always small in relation to the size of the turbulent eddies. Because eddy size scales with height above the surface, anemometers with short path lengths are required close to the ground. A "rule-of-thumb" to avoid significant high-cut frequency corrections is for the path length to be 1/20 times the measurement height (e.g., using an anemometer with a 15 cm path length only at heights greater than 3 m), though Kristensen and Fitzjarrald (1984) show reasonable flux measurements down to only a few times the height using single-axis (vertical) sonic anemometers. Van Dijk (2002) later modified this conclusion to show that three-dimensional sonic anemometers (currently in use) have more path averaging and need to be deployed at higher position than had been previously recommended. Similarly, the path length in open-path CO_2-H_2O sensors (see below) and the separation between anemometer and scalar sensor or inlet dictate minimum height-above-surface specifications.

2.4 Eddy CO_2/H_2O Analyzer

2.4.1 General Description

The second component of a system to determine CO_2 and water-vapor fluxes is a fast-response analyzer for measuring turbulent fluctuations in CO_2 and H_2O molar concentrations at high frequency. Currently, most sites use a nondispersive infrared absorption analyzer (commonly referred to as infrared gas analyzer – IRGA), in either an open- or closed-path configuration. The relative advantages and disadvantages of these systems will be discussed in Sect. 2.4.4. For either system, the measurement scheme consists of a broadband IR light source, band-pass filters (rather than a monochromator or other *dispersive* device to select wavelength) to select a wavelength range that spans absorption lines for CO_2 and water vapor, and a detector. Light is absorbed by CO_2 and H_2O in the light path, and the reduced intensity observed by the detector is a nonlinear function of the molar concentration of CO_2 and H_2O. A closed-path analyzer has an internal sample cell (optical bench) that is flushed by sampled air while in open-path sensors the sample cell is in the open air. In order to account for variations in the light source intensity and detector response, light absorption is evaluated by comparing the detector signal with a reference signal. In the closed-path analyzer, the reference signal is measured using a second cell purged by a small flow of air with known (can be zero) CO_2 and H_2O molar concentration. In the open-path sensor, intensity of light at an adjacent nonabsorbing wavelength is used as reference signal.

Detector signals are converted to mixing ratios using a calibration equation and constants (see Sect. 3.2.1.2) and accounting for density of air at pressure and temperature in the sample cell. In open-path analyzers, temperature and pressure vary with ambient conditions, so their fluctuation has to be accounted for through the so-called Webb-Pearman-Leuning (WPL) density corrections (Webb et al. 1980, Sect. 4.1.4.2). In closed paths, temperature and pressure within the sample cell are different from the ambient conditions but can be precisely controlled to constant values, reducing the need to account for temperature fluctuations in the WPL density correction. In both systems, however, the dilution correction should take water vapor fluctuations into account (Sect. 4.1.4.4).

In addition to dilution effects, a correction for spectral interference should also be considered. The underlying spectroscopic details of this are beyond the scope of this chapter, but the proportionality between light absorbance and density depends on the temperature, the pressure and the composition of the sample matrix, especially its water content. At higher mixing ratios, the gain (change in absorbance for a unit change in density of the analyzed gas) tends to decline (in part due to band broadening). McDermitt et al. (1993) derived a calibration function for IRGAs based on nonoverlapping line approximation that includes the influence of pressure, temperature, and water vapor on the CO_2 signal and assuming broadening coefficients for dry air. This correction is generally incorporated in factory calibrations and should not be introduced in the standard data treatment. If very accurate absolute CO_2 mixing ratios are required, the application of this equation to raw signals would be recommended (Sect. 2.4.2.3). In any case, it is important to realize that temperature and pressure fluctuations affect the computed mixing ratio so that they are held to a minimum. Water vapor fluctuations affect computed mixing ratios as well and need to be quantified both to compute the water-vapor flux (latent heat) and to accurately account for the water vapor affect on CO_2 mixing ratio by the spectral corrections included in factory calibration and the dilution corrections applied in data processing.

2.4.2 Closed-Path System

2.4.2.1 Absolute and Differential Mode

Closed-path system may run in either *absolute mode*, if the reference has zero CO_2 and H_2O concentrations, or *differential mode***,** if the reference has constant molar concentrations near ambient conditions. In absolute mode, dry CO_2-free, purge gas is achieved using a cylinder of compressed nitrogen or CO_2-free air, a purge-gas generator, or chemical scrubbers in line with a compressor pump. In the latter case, this requires some attention to replenish as they are used up. In differential mode, a cylinder of compressed gas of required mixing ratio is needed. Operationally, absolute mode is simpler, but if the analyzer zero is being recorded as part of routine calibration (see below), the data recording must span a wide range from zero to >400 ppm CO_2. For either mode of operation, the flow rate necessary to purge the reference cell is typically only a few $cm^3 min^{-1}$, so gas cylinders can last a long time or power requirements for compressors or zero-air generators are modest. But, if routine calibration includes a zero check, the capacity of the purge-gas source to deliver adequate flow rates to flush the sample cell must be considered. In differential mode the data only span a narrow range centered on the ambient mean mixing ratio; for applications using analog-to-digital converters for data logging this allows better signal resolution.

2.4.2.2 Tubing Requirements for Closed-Path Sensors

A closed-path sensor needs to have sample air brought to it. The presence of tubing introduces possibility for chemical and physical alteration of the air as well as attenuation of high-frequency variation. The following requirements are given to minimize these artifacts and limit the magnitude of correction terms:

1. Minimize attenuation of high-frequency variability throughout the sampling system
2. Avoid water condensation within tubes and analyzer
3. Avoid pressure fluctuations and air contamination caused by the pump
4. Comply with the analyzer range of operational parameters
5. Stabilize and monitor the air flow
6. Keep the analyzer chamber clean
7. Avoid generation or loss or the analytes of interest (artifacts)

Air transport through the tube has two main consequences on the measurements: First, the sampling of CO_2 concentration lags that of wind velocity, which has to be accounted for in covariance computation (Sect. 3.2.3.2); secondly, diffusion and physical mixing of the sample stream as air passes through the inlet tubing attenuate high-frequency fluctuations in mixing ratios. In laminar flow conditions ($Re < 2{,}100$, where $Re = \frac{2Q}{\pi r_t \nu'}$ is the Reynolds number, Q is air flow in the tube, r_t is tube radius, and ν is kinematic viscosity of air), a parabolic velocity profile is established with a maximum velocity at the center of the tube that is twice the average velocity of air through the tube. The sample arriving at the CO_2 analyzer is thus a mixture of air that entered the tubing at different times and atmospheric fluctuations are smeared out. The velocity profile for turbulent flow is more constant across the tubing cross section with only a very thin boundary layer at low velocity adjacent to the tubing wall; so there is less physical mixing due to the velocity shear. Thus, choosing the inlet diameter and flow rate to maintain the Reynolds number above a threshold of 3,000–3,500 for maintaining turbulent flow is desirable (Lenschow and Raupach 1991; Leuning and King 1992) to minimize the loss of high-frequency fluctuations by passing through an inlet line (Leuning and King 1992). However, power limitations or site configurations sometimes may preclude achieving a high enough flow rate to maintain turbulent flow. In these conditions, specific corrections for high-frequency losses are required (Sect. 4.1.3.2) and data quality may suffer if the correction magnitude is too large. Even though turbulent flow reduces the physical mixing of sample air, other mechanisms including adsorption of analyte on the tubing wall and mixing induced by fittings and bends in the tubing may still attenuate high-frequency fluctuations; so it is always essential to evaluate the spectra and cospectra to detect anomalies at high frequency and, when necessary, apply appropriate corrections (Sect. 4.1.3.2).

Recommendations for Set Up

The ideal set up consists in an inlet placed as close as possible to the sonic averaging volume, a sampling tube, a mass flow controller, the analyzer, and the pump (Fig. 2.8). The pump needs to be downstream of the analyzer to preserve the variability in mixing ratio, but pressure pulsing from the pump operation must be avoided. This is easily accomplished by including a ballast volume (B) between the analyzer and pump. Operating the analyzer at negative pressure, ∼25 kPa below ambient is recommended. Filters are necessary to protect the detector cell from damage by debris or particles and reduce accumulation of material on the tubing walls that may absorb/desorb CO_2 or water vapor. It is recommended to place two filters, a first one at the inlet and a second one near the analyzer for additional protection. For the inlet filter, Teflon© membranes (e.g., Pall Zefluor 47 mm diam, 2 μm pore size, Gelman ACRO 50, 1 μm pore size) in an open-face filter holder are a good option. Because Teflon© is hydrophobic it makes a good barrier to liquid water and does not itself interact with the water vapor in the atmosphere. Accumulated dirt on the filter may interact with water, so changing filters regularly is required even if they are not becoming clogged. The second filter (e.g., Gelman inline Teflon©disk filter) is installed close to the analyzer as a final protection against dirt or liquid water entering the detector cell.

Dead volumes, sharp bends, and restrictions in the tubing between the inlet and the analyzer promote mixing and will further attenuate high-frequency fluctuations. They should be minimized as much as practical by selecting properly sized fittings and configuring plumbing so that smooth curves rather than 90° elbows are possible.

In addition, the tubing material must be considered. Aside from the obvious need to be impervious to damage from UV radiation and possible exposure to extreme temperatures (e.g., polyethylene becomes brittle in cold temperature), the tubing must not interact with the compounds being analyzed. CO_2 is fairly inert on dry surfaces, but H_2O is particularly reactive and tends to equilibrate with surfaces so that ambient fluctuations in its mixing ratio are attenuated by passing through a tube. Hydrophobic materials such as Teflon,© polyethylene, and Synflex are the best choices to minimize wall absorption, but accumulated dust and coatings of semivolatile organics can also absorb water; so keeping the tubing clean by using a filter at the inlet and cleaning or replacing the tubing periodically should be planned.

Finally, when using an inlet tube it is important to avoid conditions that allow condensation anywhere along the path to the analyzer. For example, water vapor may condense in the tubing if it passes through an air conditioned room and outdoor temperature and relative humidity are high. Or in another common example, when the above canopy environment is warm and humid and the analyzer is at the base of the tower with dew-point temperatures. Heating the sample line to maintain temperatures above the ambient dew point at all points or reducing the pressure in the tubing so that the partial pressure of water vapor does not exceed saturation will prevent condensation.

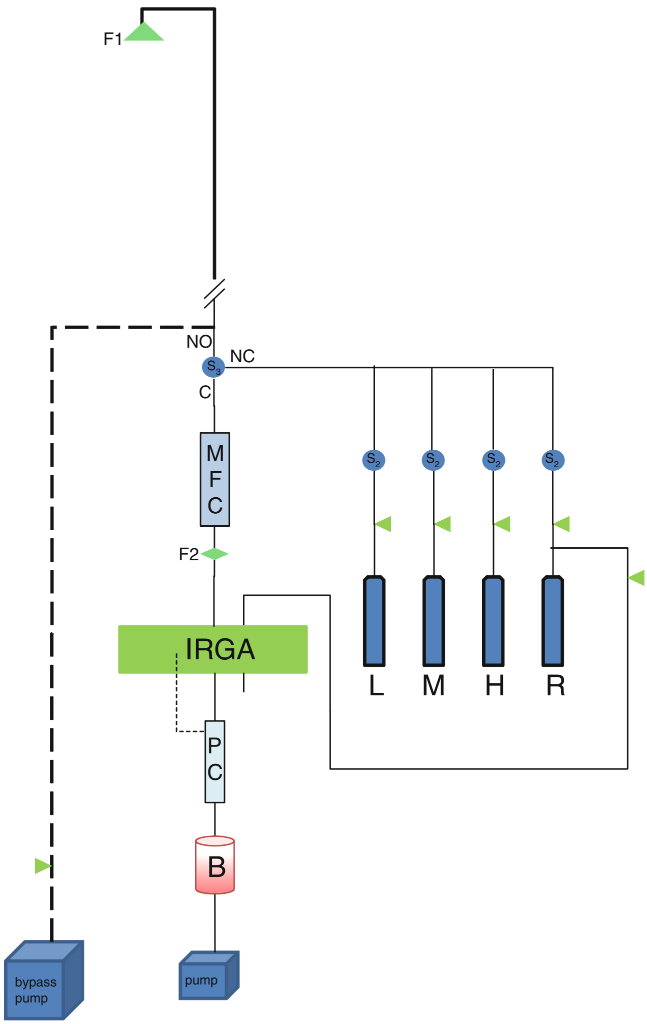

Constraints on Tube Dimensions and Mass Flow

Mass flow (Q), tube length (L_t), and radius (r_t) should be dimensioned in order to reach the best compromise providing the highest Reynolds number, Re and the shortest lag time, $t_l = \frac{L_t \pi r_t^2}{Q}$ possible, while minimizing the pressure drop in the analyzer chamber, $\Delta p \lesssim 8 \frac{Q L_t \rho \nu}{\pi r_t^4}$ (using laminar flow as a lower limit).

This implies conflicting constraints on Q and r_t (higher mass flows and lower radius will lead to larger Reynolds numbers and lower lag time but also to higher pressure drops and the need for larger pumps). This clearly indicates the need to reduce the tube length and thus to place the analyzer as close as possible, that is, a few meters, from the tube inlet. When the sampling point is above a tall canopy (e.g., forests), this would mean placement on the tower and would require a more elaborate environmental enclosure to protect the instrument from weather and environmental variability. However, in this case, the system to access would be more difficult, which would impede maintenance and calibration. An alternative would be to place the analyzer at ground level, to flow the air from the canopy top to the ground at high mass flow (e.g., $>10\,\mathrm{l\,min^{-1}}$) through a large radius tube, in order to maximize *Re* without unduly increasing Δp, and to divert a portion of this flow through the analyzer from a junction close to the analyzer at a mass flow sufficient to flush the detector cell. Manually adjustable flow valves or active pressure and flow controllers are required to balance the bypass and sample flows and to maintain cell pressure at the desired values (Fig. 2.8).Whatever the set up that is chosen, a careful analysis of flux cospectra is necessary in order to apply the most relevant high-frequency correction to the flux (Sect. 4.1.3).

To avoid changes in cell pressure and lag times as conditions change (temperature, accumulating dirt on filters, and aging of pumps affect pressure and flow) inclusion of active pressure and flow control elements (mass flow controller) is recommended rather than using manually adjusted restrictions (e.g., needle valves) to set the desired pressure and flow (Fig. 2.8).

Fig. 2.8 Schematic of a CO_2 analyzer configured for a 3-point calibration with zeroing check. Option for bypass flow is indicated by *dashed line* connecting to Bypass pump. Inlet and in-line filter are designated by F1 and F2. S_3 indicates a 3-way switching valve with the Common, Normally Open, and Normally Closed ports marked as C, NO, and NC that is used to select whether the analyzer gets sample or calibration standard. Two-way valves (shutoff) on the calibration gases, indicated by S_2, select which calibration gas is in use. Solenoid valves controlled by a data logger would allow the calibrations to be automated, or they could be performed manually. The cylinder indicated by R would be filled with a gas mixture having approximately ambient CO_2 to operate in differential mode or CO_2-free air (optionally N_2) from a cylinder or produced by a CO_2 scrubber to operate in absolute mode. Flow adjusters/restrictors are designated by *green triangles*. The restrictors on the calibration gases limit the flow so that the mass flow controller (*MFC*) does not have to overcome a sudden change from subambient pressure during sampling to high pressure from the compressed gas standards. Frits, capillaries, or needle valves are suitable devices for the control elements. The *line* from cylinder R to the IRGA is connected to the reference cell and has a restriction to limit its flow to the minimum needed to purge the cell. A pressure controller downstream of the IRGA is used to maintain constant pressure in the sample cell. Either an integrated pressure controller that combines pressure transducer, electronics, and controlling valve, or a separate controller with input from a transducer on the detector cell could be used. A ballast (B) between analyzer and pump damps the pressure and flow oscillations induced by the pump. A control element is shown upstream of the bypass pump to adjust its flow as necessary to achieve the desired overall flow and pressure

2.4.2.3 Calibration for CO_2

Individual instrument calibration constants are derived by fitting the calibration function (McDermitt et al. 1993) to a series of known and traceable standards. The approximations underlying the calibration fit are best met at CO_2 mixing ratios below 1,100 ppm and the temperature and pressure corrections are most accurate below 500 ppm, which is adequate for typical ambient concentrations. In fact, the resolution of the instrument can be enhanced if the calibration is constrained to the range of expected ambient values (350–650 ppm), rather than the full range of the analyzer, which is often 0–3,000 ppm. For eddy covariance fluxes, the mean mixing ratios are subtracted from the observations rendering accuracy of absolute mixing ratios less important than accurate determination of the turbulent fluctuations. Hence, the slope of the calibration curve near the observed mixing ratio rather than the intercept term is most critical. However, the nonlinear response must still be correctly accounted for unless fluxes will be biased because fluctuations in mixing ratio above and below the mean will cause disproportionate instrument response. Even so, increasing the absolute accuracy of mixing ratios adds value to the EC estimates through supplemental activities that can provide additional process-level understanding, for example, advection and transport studies, and enhance scaling activities, for example, inverse modeling; so it is beneficial to make the best calibration that can be achieved with available resources.

The cell pressure and temperature of the gas being analyzed are part of the calibration equation. While these are measured by the analyzer, it is important to realize that the pressure and temperature sensors only measure one point in the analyzer, not necessarily the sample gas that is in the cell. It is essential to minimize temperature and pressure differences between sample and calibration modes and to reduce fluctuations in T and p that induce gradients in the analyzer such that measured T and the conditions within the cell diverge. Enhancing the thermal management and pressure control of the instrument beyond factory defaults provides better analytical results. Protecting the analyzer from solar heating or rapid temperature cycling by air conditioning and heating is a simple minimal step. Ideally, placing the analyzer in a temperature-controlled enclosure that maintains the instrument housing at a relatively stable temperature is the best option. If the analyzer is well calibrated and operated according to the design specifications, the results from internally computed mixing ratio are generally quite accurate. However, there is no substitute for periodic measurement of field calibration standards with traceable known mixing ratios to confirm the accuracy of the instrument's calibration curve and detect problems. A multipoint calibration with at least three points spanning the range of ambient mixing ratio is necessary to verify that sensor nonlinearity is correctly compensated and assure absolute accuracy. Over the typical range of ambient concentrations in the atmosphere, a third-order polynomial, constrained to that range, is adequate to compute CO_2 mixing ratios to better than 0.1 ppm accuracy (Ocheltree and Loescher 2007, Fig. 2.3). If an automated field calibration is being used for closed-path sensors, it is also prudent to have it cycle on intervals that are not even fractions of a day so that the time series is not biased by always removing data at the same time each day.

If a highest absolute accuracy in CO_2 mixing ratios is required, it is best to record raw signals and compute mixing ratios based on calibration against known standards. One important practical consideration is that the dilution gas for CO_2 standards must be air. Using other gases such as N_2 or even synthetic air that has an O_2/N_2 ratio very different from ambient air affects the shape of absorbance bands and violates the simplifying assumptions behind the McDermitt et al. (1993) calibration equation. Although in practice the deviation is small, it should be noted that the IR absorption lines selected in broadband absorption gas analyzers primarily cover the $^{12}CO_2$ lines. Ambient measurements at ^{13}C: ^{12}C isotopic ratios very far from typical ambient levels or calibration against CO_2 standards with isotopic ratios very different from ambient (say, CO_2 from fossil fuel sources) can lead to mixing ratio errors of a few 0.1 ppm. For flux measurements this uncertainty will be inconsequential, but it is a consideration for accurate absolute mixing ratio measurements.

2.4.2.4 Water Vapor Calibration

Water vapor calibration cannot rely on compressed gas standards because gas mixtures with stable water vapor mixing ratios are not available. Dew-point generators, which bubble a flow of air through a temperature-controlled volume of water deliver air with a known water vapor pressure and are used to manually calibrate the H_2O channel of IRGAs (Loescher et al. 2009). It is important to operate the dew-point generator within flow conditions at which the air stream will achieve thermal equilibrium with the water chamber, and avoid deviations in pressure that would affect the resulting saturation vapor pressure of water. An alternative to direct calibration of H_2O is to provide a secondary measurement of absolute humidity (e.g., using a chilled mirror (Loescher et al. 2009)) or compute absolute humidity from ambient temperature and relative humidity measured independently.

The accuracy of water vapor calibration affects the accuracy of measured CO_2 mixing ratios and fluxes through the dilution corrections and WPL term (Sect. 4.1.4) Water vapor corrections are obviously critical for accurate CO_2 flux measurements because H_2O and CO_2 fluxes are typically correlated.

2.4.3 Open-Path Systems

2.4.3.1 Installation and Maintenance

The larger physical size of an open-path sensor than the inlet filter for closed-path analyzer presents a flow obstruction. The open-path sensor needs to be far enough away from the SAT that its flow distortion does not interfere with the wind measurement, but not so far that the sensor separation exceeds criteria for minimizing spatial-averaging problems (see Sects. 2.3.3 and 4.1.3.2). As noted above, the separation distance needs to be smaller than the turbulent eddies, and the minimum physical separation that can be achieved sets a lower limit on the height the sensor can be used above the surface without unreasonable loss of high-frequency covariance with the wind. The cospectra should be examined for evidence of high-frequency loss and correction terms evaluated to ensure that their magnitude is reasonable. Accumulated dirt, precipitation, or ice on the sensor windows prevents its operation. To reduce instrument down time, the sensor should be tilted from vertical orientation to promote rapid runoff of droplets. The sensor windows need to be wiped periodically to remove accumulated dust following manufacturer-recommended protocols.

2.4.3.2 Calibration

For open-path sensors, automated routine calibrations are not practical. Periodic manual calibration by purging a chamber placed over the sensor path with gas mixtures having a known CO_2 is possible. It is challenging to ensure a good seal that prevents mixing of outside air with the calibration standard without causing pressure perturbations inside the housing. Alternatively, a secondary calibration by comparison to simultaneous measurements by a second well-calibrated analyzer (e.g., profile CO_2 analyzer, see below) is a reasonable solution that could meet the accuracy requirements for a flux measurement. Regular manual calibrations of open-path sensors using a consistent protocol can help to assure reliable data and detect instrument problems, but the accuracy of open-path calibrations will not match what can be achieved for a closed-path sensor.

2.4.4 Open and Closed Path Advantages and Disadvantages

Open- and closed-path sensors each have advantages and disadvantages. A closed-path sensor can be configured to precisely control temperature and pressure of the sample gas, reducing a potential source of imprecision and avoiding the need to account for covariance in air density and water vapor by including large density correction terms (see Sect. 4.1.4). Secondly, it is straightforward to implement routine automated calibrations supplying known standards to the analyzer to verify the measurement accuracy and precision. The performance of the closed-path sensor is not degraded by adverse weather conditions. A drawback to closed-path sensors is that the necessity of an inlet line induces an attenuation of high-frequency variations and also introduces some delay between when a parcel of air enters the inlet and when it reaches the analyzer. The high-frequency attenuation was discussed in Sect. 2.4.2.2. Corrections for this effect are presented in Sect. 4.1.3. The delay, lag time, must be accounted for when computing covariance between the mixing ratios and vertical wind velocities (see Sect. 3.2.3.2), and is dependent on flow rates and pressure, though it can be determined quite accurately by computing the lagged covariances between CO_2 or H_2O and vertical wind speed or temperature and selecting the time offset that gives the maximum correlation coefficient. The lag for CO_2 and H_2O would be identical if they had no wall interaction. In practice, H_2O tends to stick to the tubing walls more, but large differences in lag are evidence that the tubing or filter is contaminated by hydrophilic material and should be replaced or cleaned. Computing lagged correlations over time to detect changes is a simple and effective measurement quality check.

If high-frequency response or power requirement were the only considerations, open-path sensors would be an ideal solution. However, the gain in high-frequency response and reduced power is made at the expense of increased down time (from rain and inclement weather), and the need to include heat fluxes in the calculation of CO_2 and H_2O fluxes (Chap. 4) (Leuning 2007; Webb et al. 1980; Massman 2004), Leuning 2004), which add additional uncertainties (Chap. 7). Sensor self-heating (or radiational cooling) (Sect. 4.1.5.2, Burba et al. 2008,) may require a correction term and adds additional uncertainty to CO_2 fluxes measured by an open-path sensor that is oriented vertically. Haslwanter et al. (2009) found in a long-term comparison of collocated open and closed-path sensors that there was little overall difference in flux uncertainty. However, when using an open-path sensor for actual fluxes close to zero (no flux), the WPL and Burba corrections can sometimes be several orders of magnitude larger than the flux making estimates of uncertainty (1) among temporal scales, (2) among sites with contrasting conditions, and (3) across different technologies difficult to quantify. Finally, spatial averaging due to sensor path length and separation from the anemometer introduces unacceptable uncertainties in flux for measurement heights too close ($h_m < \sim 3$ m) to the surface. Selection between these two technologies should be based on logistical considerations, individual research requirements, and site characteristics. At sites with frequent precipitation, or large heat fluxes, the improved frequency response by open-path analyzers may not be an acceptable tradeoff. Some research objectives, such as process-based studies as opposed to those needing annual averages, can be accommodated by constraining the collection period to times when the uncertainties imposed by open-path environment are well understood and acceptably small.

The drawbacks of closed-path sensors are minimized by placing the analyzer near the inlet with very short lengths of tubing, but this requires additional engineering to provide adequate protection of the analyzer from weather and temperature variation in the harsh outdoor environment on top of a tower, which would not be needed for analyzers inside a building. On triangular towers, engineering requirements include secure mounting, but it has been successfully accomplished even in the hot, humid tropics. On scaffold towers, mounting is simplified and some protection from precipitation and solar radiation is provided by placing analyzer boxes below the top stage.

A novel CO_2 sensor that was first released in 2010 provides an integrated package with a CO_2 sensor based on open-path technology but enclosing the path may be an excellent alternative to either existing open or closed-path analyzers. The enclosure includes fast temperature and pressure sensors and is flushed by an integrated low-power flow module. This hybrid allows measurements with a minimal inlet and provides electronics intended for outdoor installation without the need for additional environmental control or user modification. The instrument specifications appear to be ideal for flux measurement, but so far it has not been in use long enough to evaluate its actual performance. The short (1–2 m) inlet tube separates the inlet located near the sonic path from the analyzer cell and electronics and is also intended to attenuate ambient temperature fluctuations, thus reducing the density correction term associated with temperature. Additionally, this inlet provides an ideal point to introduce calibration gases by supplying them through a "tee" in excess of the sample volume required.

2.4.5 Narrow-Band Spectroscopic CO_2 Sensors

An emerging alternative to broadband absorbance instruments is a new class of analyzers based on laser spectroscopy. Lasers provide light that can be tuned to very narrow frequencies and modulated to scan across individual lines in the IR absorbance spectra of CO_2 and H_2O. Fitting the observed spectra to well-known line strength data bases provides a signal that is nearly linear with respect to the density of CO_2 and H_2O. In practice this method still requires some calibration to account for nonideality and drift in the laser frequency output, but with significantly reduced frequency and complexity. These laser-based spectrometers achieve very long path length by employing multipass cells (Herriott) or very high reflectivity mirrors that keep most of the light inside the cell. Cavity ring down injects a short laser pulse into a high reflectivity cell and observes the decay of every small fraction of light that "leaks" out through a small aperture. The signal of interest is the duration of light pulse coming from the cell rather than its absolute intensity, τ being the transit time for light at each wavelength, rather than the absorptance. Rapid firing of the laser provides many individual measurements that are signal averaged to reduce noise and the laser frequency is modulated to scan across the absorbance spectra (Richman et al. 2004). Another alternative is an integrated cavity, which also uses very high reflectivity (but not 100%) mirrors but does not have a defined exit for the light to reach the detector. Instead the very small fraction of light transmitted through one of the mirrors is collected and its intensity is measured as the wavelength is modulated across the absorbance feature. The light that is detected at any instant in time spans the range of wavelengths that have been injected since the scan started. Sophisticated data processing algorithms incorporated in the analyzer's software deal with this. These technologies are also pioneering a wide range of new applications and measurement capability for other gas species (including isotopic discrimination) with better accuracy, precision, and resolution than can be obtained by traditional broadband IR absorbance. In principle, these systems when configured with small detector cells flushed by high volumetric flow would be ideal sensors for eddy covariance flux measurements of CO_2 as well as other species. By selection of nearby absorbance bands for different species accessed in single scan or using dual lasers these spectrometers can simultaneously measure more than one constituent. Possibilities are limited only by availability of lasers at the wavelengths of interest and time delays for tuning between different frequency regions or multiplexing different lasers. An optimum combination would include high-frequency measurement of both H_2O and CO_2 (or another scalar) because water vapor covariance is essential to account for density fluctuations. The laser spectrometer-based analyzers are also closed-path instruments, so the same considerations about tubing materials, flow rates and pressures that were described in Sect 2.4.2.2 will apply.

2.5 Profile Measurement

Net ecosystem exchange cannot be determined by eddy flux alone, but requires measurement of the storage term, (Sect. 1.4, Eq. 1.19, see also Loescher et al. 2006b). From Eq. 1.19, term I, the storage term, $\int_0^{h_m} \overline{\rho_d} \overline{\frac{\partial \chi_s}{\partial t}} dz$ appeared as the vertical integral of concentrations time derivatives. Note that the vertical integral of concentrations is equivalent to finding the column-average concentration and the storage could be quantified by continually measuring from perfect mixing inlet manifold that drew air equally from all heights, or using a long-path instrument that observed total CO_2 density between the ground and sensor height instantaneously. However, it is difficult to ensure perfectly balanced sampling, and there is often useful ecological information in the shape of and changes in the concentration profile. Instruments with open paths a few to 60 m long are not commercially available, and would be difficult to deploy in most canopy situations where vegetation would obstruct the path. The number of measurement levels required to accurately quantify the mixing ratio profile depends on canopy complexity and height. Profile accuracy for observations in a mature deciduous forest was evaluated using data records from the Harvard Forest Main tower. Figure 2.9 shows the difference in CO_2 profile when one of the 8 measurement heights is deleted. Papale et al. (2006) also showed that the difference between storage estimates based on a single point and a complete profile could induce, at forested sites, differences up to 25 gC m^{-2} year^{-1} on NEE, to 80 gC m^{-2} year^{-1} on total ecosystem respiration (TER) and to 100 gC m^{-2} year^{-1} on gross primary production (GPP). Measurement levels below the canopy top are thus essential to accurately fit a profile and correctly evaluate the storage term. Removing one above-canopy measurement level produced $<1\%$ uncertainty in annual NEE estimates. There was much larger uncertainty, however, when removing a measurement level below the canopy, that is, 20–60%, in the ability to detect individual events at the 30-min timescale, for example, sweeps and ejections. The timescale of profile measurements used to quantify canopy storage needs to match the integration time for the eddy covariance fluxes, that is, 30-min. What has to be determined is how many complete column samples are needed to best characterize the column estimate for any particular 30-min average. Often the differences in concentration from the EC measurement

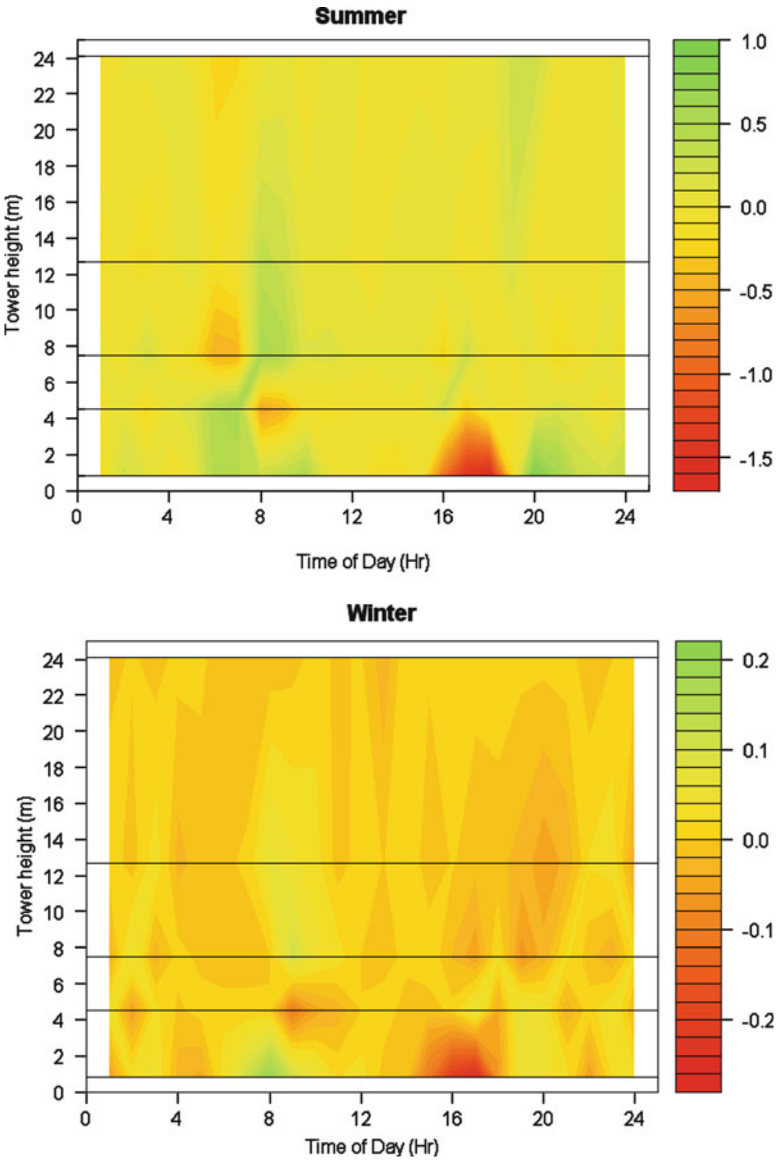

Fig. 2.9 Differences in CO_2 concentration profiles when one measurement level is removed. Data are from 2004–2008, Harvard Forest, main tower at 30-min increments at 0.3, 0.8, 4.5, 7.5, 12.7, 18.3, 24.1, and 28 m heights, with $n = 31{,}142$ for summer and winter seasons, respectively. We assessed the impact of removing the 4.5, 7.5, 12.7, and 24.1 m measurement levels on the CO_2 profile (0.3, 18 and 28 m heights were always fixed for both observed and predicted estimates). For each case, a generalized boosting model (gbm) was fit to the data from the tower heights, while one measurement level was excluded. Then the observed measurements from all heights were assessed against the gbm model fits. The difference between the observed data and the prediction from the model fit was computed using the following statistic; $\textit{loss of fit} = ((\textit{observed} - \textit{predicted})^2)^{0.5}$. CO_2 units are μmol m^{-2} s^{-1}, and we assumed normal distribution

height and the ecosystem floor can be very small under well-mixed conditions or very large when a plant canopy is decoupled from the above-canopy environment. Accurately detecting these differences is best done with a single analyzer, hence removing any among-sensor biases. When profile levels are sampled sequentially, the time offset between measurements at each level will need to be accounted for in computing the storage term, usually by some averaging or interpolation to arrive at some estimate of the average concentration profiles during successive intervals. There is typically a settling time for the analyzer to equilibrate after switching from one sample to another, which can be estimated using Allan's variance techniques (Allan 1966). Reducing the transit time and switching delay for profile sampling can be achieved by consistently pulling all the profile inlets, each with the same volume (and resistance) through a common large volume manifold, and then subsampling each profile measurement through the analyzer. The profile analyzer requires the same considerations about condensation and environmental control as the eddy analyzer.

The measurement of the concentration profile, because it can operate with reduced flow rates compared to EC, may operationally be easier to calibrate as an absolute measurement of the mixing ratio without consuming large volumes of expensive standards. For systems with frequent and easy operator access manual approaches based on supplying an excess flow of calibration standard at an inlet are an alternative to built-in calibration systems. An advantage of having good absolute calibration of a profile system is that it provides a secondary calibration of the eddy system by selecting the data from periods when the profile system takes sample from the same location as the eddy system.

2.5.1 Requirements for Measurement Levels

The number of profile levels required is dictated by the need to adequately resolve the vertical gradients in scalar quantities and adequately represent the shape of the vertical profile. Increasing height and complexity of the canopy requires more levels. Dense canopies impede vertical mixing, allowing larger concentration gradients. Vegetation strata will affect the magnitude and shape of the vertical profile and need to be considered in placing the sampling heights.

The number of measurement levels on a tower will differ among different types of ecosystem structure. There should be at least 4 measurement levels over short-stature ecosystems, grasslands, croplands, etc., and where possible, the bottom level (closest to the ground, Level 1) measuring within the canopy environment. The location of the remaining measurement levels (the distance between Level 1 and the tower top) should be mounted equal distance apart (arithmetic not logarithmic scale) over these short stature ecosystems. For shrublands, and open- and closed-canopy forests, there should be a minimum of 2 measurement levels above the canopy, which includes measurements at the top of the tower. There are no absolute criteria to determine the level closest to the canopy (but above the canopy). It will be dependent on local scalar source and sink status of individual canopies, surface roughness, and topography to best capture the vertical divergence between this measurement level and the well-mixed layer at the top of the tower. The next lower level should be associated with mean canopy height and region with the highest leaf area density. Placement of other measurement levels below-canopy should capture other ecologically significant strata, for example, established understory plant canopy.

Determining the measurement height of lowest level will be challenging at sites with significant snow accumulation. The ideal measurement height for growing season may be buried by winter snow, requiring some adjustment of sensor height and careful documentation.

2.5.2 Requirements for Profile Mixing Ratio Measurement

Analysis of profile mixing ratios is subject to the same concerns given above for the eddy analyzer. Instead of single sample line, multiple inlets, each with an inlet filter, would be brought to a manifold or stream select valve. The analyzer is connected to the outlet of inlet manifold and the profile inlets are opened one at a time. Analyzer output immediately after switching to a new level will need to be discarded due to pressure transients from the valve switching and to allow the inlet to be flushed with air from the selected inlet. If power is not limiting, the selection hub can be configured to allow the inlets not in use to be continually flushed by pulling on them through a bypass pump. The switching time between levels is reduced by maintaining as high a flow through the inlet as practical. A bypass flow with small subsample to the analyzer can be used to rapidly flush the inlet without needing a high flow through the analyzer itself. Furthermore, operating the inlet at a higher flow provides the reduced pressure to prevent condensation inside the tubing. To avoid artifacts due to pressure differences for each inlet height, a pressure controller should be used on the profile system

Acknowledgments J. W. Munger was supported by Office of Science (BER) U. S. Dept of Energy DE-SC0004985, and H.W. Loescher and H. Luo were supported by National Science Foundation DBI-0752017. The authors wish to thank P. Duffy for statistical support on the profile analyses.

References

Akabayashi S, Murakami S, Kato S, Chirifu S (1986) Visualization of air flow around obstacles in laminar flow type clean room with laser light sheet. Paper presented at 8th international symposium on contamination control, Milan, Italy, Sept 9–12

Allan DW (1966) Statistics of atomic frequency standards. Proc IEEE 54:221–231

Arya SPS (1988) Introduction to micrometeorology. Academic, San Diego

Barthlott C, Fiedler F (2003) Turbulence structure in the wake region of a meteorological tower. Bound Layer Meteorol 108:175–190

Burba GG, Anderson DJ, Xu L, McDermitt DK (2008) Correcting apparent off-season CO_2uptake due to surface heating of an open path gas analyzer: progress report of an ongoing study. LI-COR Biosciences, Lincoln

Campbell GS, Unsworth MH (1979) Inexpensive sonic anemometer for eddy correlation. J Appl Meteorol 18(8):1072–1077

Cermak JE, Horn JD (1968) Tower shadow effects. J Geophys Res 73(6):1869–1876

Chen J, Franklin JF, Spies TA (1990) Microclimatic pattern and basic biological responses at the edges of old-growth Douglas-fir stands. Northwest Environ J 6(2):424–425

Chen J, Franklin JF, Spies TA (1992) Vegetation responses to edge environments in old-growth Douglas-fir forests. Ecol Appl 2(4):387–396

Chen J, Franklin JF, Spies TA (1993a) An empirical model for predicting diurnal air-temperature gradients from clearcut-forest edge into old-growth Douglas-fir forest. Ecol Model 67:179–198

Chen J, Franklin JF, Spies TA (1993b) Contrasting microclimatic patterns among clearcut, edge, and interior area of old-growth Douglas-fir forest. Agric For Meteorol 63(3–4):219–237

Culf AD, Fisch G, Hodnett MG (1995) The albedo of Amazonian forest and ranchland. J Clim 8:1544–1554

Culf AD, Esteves JL, Marques Filho ADO, da Rocha HR (1996) Radiation, temperature and humidity over forest and pasture in Amazonia. In: Gash JHC, Nobre CA, Roberts JM, Victoria RL (eds) Amazonian deforestation and climate. Wiley, Chichester, pp 175–191

Dabberdt WF (1968) Wind disturbance by a vertical cylinder in atmospheric surface layer. Bull Am Meteorol Soc 49(7):767–771

Davies ME, Miller BL (1982) Wind effects on offshore platforms – a summary of wind tunnel studies. Rep., National Maritime Institute, Feltham

Detto M, Katul GG, Siqueira M, Juang J-Y, Stoy P (2008) The backward-facing step flow analogy revisited. Ecol Appl 18:1420–1435

Dyer AJ (1981) Flow distortion by supporting structures. Bound Layer Meteorol 20(2):243–251

Dyer AJ, Hicks BB (1970) Flux gradient relationships in the constant flux layer. Q J R Meteorol Soc 96:715–721

Foken T, Leclerc MY (2004) Methods and limitations in validation of footprint models special issue on footprints of fluxes and concentrations. Agric For Meteorol 127(3–4):223–234

Gash JHC, Dolman AJ (2003) Sonic anemometer (co)sine response and flux measurement I. The potential for (co)sine error to affect sonic anemometer-based flux measurements. Agric For Meteorol 119(3–4):195–207

Gill GC, Olsson LE, Sela J, Suda M (1967) Accuracy of wind measurements on towers or stacks. Bull Am Meteorol Soc 48(9):665–674

Göckede M et al (2008) Quality control of CarboEurope flux data – Part 1: coupling footprint analyses with flux data quality assessment to evaluate sites in forest ecosystems. Biogeosciences 5(2):433–450

Göckede M, Rebmann C, Foken T (2004) A combination of quality assessment tools for eddy covariance measurements with footprint modeling for the characterization of complex sites. Agric For Meteorol 127:175–188

Göckede M, Markkanen T, Hasager CB, Foken T (2006) Update of a footprint-based approach for the characterization of complex measurement sites. Bound Layer Meteorol 118:635–655

Haslwanter A, Hammerle A, Wohlfahrt G (2009) Open-path vs. closed-path eddy covariance measurements of the net ecosystem carbon dioxide and water vapour exchange: a long-term perspective. Agric For Meteorol 149(2):291–302

Hicks BB (1976) Wind profile relationships from wangara experiment. Q J R Meteorol Soc 102(433):535–551

Horst TW (2001) Comment on 'footprint analysis: a closed analytical solution based on height-dependent profiles of wind speed and eddy viscosity'. Bound Layer Meteorol 101(3):435–447

Horst TW, Weil JC (1992) Footprint estimation for scalar flux measurements in the atmospheric surface layer. Bound Layer Meteorol 59(3):279–296

Horst TW, Weil JC (1994) How far is enough – the fetch requirements for micrometeorological measurement of surface fluxes. J Atmos Ocean Technol 11(4):1018–1025

Horst TW, Weil JC (1995) How far is enough – the fetch requirements for micrometeorological measurement of surface fluxes (VOL 11, PG 1018, 1994). J Atmos Ocean Technol 12(2):447–447

Kaimal JC, Businger JA (1963a) A continuous wave sonic anemometer-thermometer. J Appl Meteorol 2(1):156–164

Kaimal JC, Businger JA (1963b) Preliminary results obtained with a sonic anemometer-thermometer. J Appl Meteorol 2(1):180–186

Kaimal JC, Gaynor JE, Zimmerman HA, Zimmerman GA (1990) Minimizing flow distortion errors in a sonic anemometer. Bound Layer Meteorol 53(1–2):103–115

Karipot A, Leclerc MY, Zhang GS, Lewin KF, Nagy J, Hendrey GR Starr G (2008) Influence of nocturnal low-level jet on turbulence structure and CO_2 flux measurements over a forest canopy. J Geophys Res 113, D10102, doi:10.1029/2007JD009149

Karipot A, Leclerc MY, Zhang GS (2009) Characteristics of nocturnal low-level jets observed in the north Florida area. Mon Weather Rev 137(8):2605–2621

Kormann R, Meixner FX (2001) An analytical footprint model for non-neutral stratification. Bound Layer Meteorol 99(2):207–224

Kristensen L, Fitzjarrald DR (1984) The effect of line averaging on scalar flux measurement with a sonic anemometer near the surface. J Atmos Ocean Technol 1:138–146

Leclerc MY, Karipot A, Prabha T, Allwine G, Lamb B, Gholz HL (2003) Impact of non-local advection on flux footprints over a tall forest canopy: a tracer flux experiment. Agric For Meteorol 115(1–2):19–30

Lee XH (1998) On micrometeorological observations of surface-air exchange over tall vegetation. Agric For Meteorol 91(1–2):39–49

Lemon ER (1960) Photosynthesis under field conditions. II. An aerodynamic method for determining the turbulent carbon dioxide exchange between the atmosphere and a corn field. Agron J 52(12):697–703

Lenschow DH, Raupach MR (1991) The attenuation of fluctuations in scalar concentrations through sampling tubes. J Geophys Res Atmos 96(D8):15259–15268

Leuning R (2004) Measurements of trace gas fluxes in the atmosphere using eddy covariance: WPL corrections revisited. In: Lee X, Massman W, Law B (eds) Handbook of micrometeorology: a guide for surface flux measurements and analysis. Kluwer, Dordrecht, pp 119–132

Leuning R (2007) The correct form of the Webb, Pearman and Leuning equation for eddy fluxes of trace gases in steady and non-steady state, horizontally homogeneous flows. Bound Layer Meteorol 123(2):263–267

Leuning R, King KM (1992) Comparison of eddy covariance measurements of CO2 fluxes by open path and closed path CO2 analysers. Bound Layer Meteorol 59(3):297–311

Liu HP, Peters G, Foken T (2001) New equations for sonic temperature variance and buoyancy heat flux with an omnidirectional sonic anemometer. Bound Layer Meteorol 100(3):459–468

Loescher HW (2007) Enhancing the precision and accuracy within and among AmeriFlux site measurements, expanded annual report, May 2007, DOE report

Loescher HW, Ocheltree T, Tanner B, Swiatek E, Dano B, Wong J, Zimmerman G, Campbell J, Stock C, Jacobsen L, Shiga Y, Kollas J, Liburdy J, Law BE (2005) Comparison of temperature and wind statistics in contrasting environments among different sonic anemometer-thermometers. Agric For Meteorol 133(1–4):119–139

Loescher HW, Starr G, Martin TA, Binford M, Gholz HL (2006a) The effect of local atmospheric circulations on daytime carbon dioxide flux measurements over a Pinus elliottii canopy. J Appl Meteorol Climatol 45(8):1127–1140

Loescher HW, Law BE, Mahrt L, Hollinger DY, Campbell J, Wofsy SC (2006b) Uncertainties in, and interpretation of, carbon flux estimates using the eddy covariance technique, J Geophys Res 111, D21S90, doi:10.1029/2005JD006932

Loescher HW, Hanson CV, Ocheltree TW (2009) The psychrometric constant is not constant: a novel approach to enhance the accuracy and precision of latent energy fluxes through automated water vapor calibrations. J Hydrometeorol 10(5):1271–1284

Massman W (2004) Concerning the measurement of atmospheric trace gas fluxes with open- and closed-path eddy covariance system: the WPL terms and spectral attenuation. In: Lee X,Massman W, Law B (eds) Handbook of micrometeorology: a guide for surface flux measurements and analysis. Kluwer, Dordrecht, pp 133–160

McDermitt DK, Welles JM, Eckles RD (1993) Effects of temperature, pressure, and water vapor on gas phase infrared absorption by $CO_{2.}$ Rep., LI-COR, Inc, Lincoln

Miller DO, Tong CN, Wyngaard JC (1999) The effects of probe-induced flow distortion on velocity covariances: field observations. Bound Layer Meteorol 91(3):483–493

Monin AS, Obukhov AM (1954) Osnovnye zakono- mernosti turbulentnogo peremesivanija v prizemnom sloe atmosfery. Trudy Geofiz Inst AN SSSR 24(151):163–187

Monteith JL, Unsworth MH (2008) Principles of environmental physics, 3 edn. Elsevier, Amsterdam/Boston, xxi, 418 pp

Moses H, Daubek HG (1961) Errors in wind measurements on the towers associated with tower-mounted anemometers. Bull Am Meteorol Soc 42:190–194

Munson BR, Young DF, Okiishi TH (1998) Fundamentals of fluid mechanics, 3 edn. Wiley, New York, xvii, 877 pp

Ocheltree TO, Loescher HW (2007) Design of the AmeriFlux portable eddy-covariance system and uncertainty analysis of carbon measurements. J Atmos Ocean Tech 24:1389–1409

Papale D, Reichstein M, Aubinet M, Canfora E, Bernhofer C, Kutsch W, Longdoz B, Rambal S, Valentini R, Vesala T, Yaki D (2006) Towards a standardized processing of Net Ecosystem Exchange measured with eddy covariance technique: algorithms and uncertainty estimation. Biogeosciences 3:571–583

Paw UKT, Baldocchi DD, Meyers TP, Wilson KB (2000) Correction of eddy-covariance measurements incorporating both advective effects and density fluxes. Bound Layer Meteorol 97(3):487–511

Perrin D, McMahon N et al (2007) The effect of a meteorological tower on its top-mounted anemometer. Appl Energy 84(4):413–424

Richman B, Rella C, Crosson E, Paldus B (2004) CRDS measures atmospheric CO2. Laser Focus World 40(11):S5–S7

Sanuki M, Tsuda N (1957) What are we measuring on the top of a tower? Pap Meteorol Geophys 8(1):98–101

Schmid HP (1994) Source areas for scalars and scalar fluxes. Bound Layer Meteorol 67(3):293–318

Schmid HP, Lloyd CR (1999) Spatial representativeness and the location bias of flux footprints over inhomogeneous areas. Agric For Meteorol 93(3):195–209

Schuepp PH, Leclerc MY, Macpherson JI, Desjardins RL (1990) Footprint prediction of scalar fluxes from analytical solutions of the diffusion equation. Bound Layer Meteorol 50(1–4):353–373

Schotanus P, Nieuwstadt FTM, DeBruin HAR (1983) Temperature measurement with a sonic anemometer and its application to heat and moisture fluctuations, Boundary-Layer Meteorol 26:81–93

Shinohara T (1958) On results of an experiment for practical use of the three-cup anemometers. J Meteorol Res 10:587–590

Thornthwaite CW, Superior WJ, Field RT (1962) Evaluation of an ocean tower for measurement of climatic fluxes. Publ Climatol Lab Climatol 15(3):289–351

Thornthwaite CW, Superior WJ, Field RT (1965) Disturbance of airflow around Argus island tower near Bermuda. J Geophys Res 70(24):6047–6052

Tropea C, Yarin A, Foss JF (2007) Handbook of experimental fluid dynamics. Springer, Berlin/Heidelberg, p 1557

Vaucher G, Cionoco R, Bustillos M (2004) Forecasting stability transitions and air flow around an urban building – Phase I. Paper presented at symposium on planning, nowcasting, and forecasting in the Urban Zone, 84th AMS Meeting, Seattle, 11–15 Jan 2004, American Meteorological Society, Boston, MA

van Dijk A (2002) Extension to 3D of "The effect of line averaging on scalar flux measurements with a sonic anemometer near the surface" by Kristensen and Fitzjarrald. J Atmos Ocean Tech 19:80–82

Webb EK, Pearman GI, Leuning R (1980) Correction of flux measurements for density effects due to heat and water-vapor transfer. Q J R Meteorol Soc 106(447):85–100

Whitaker S (1984) Introduction to fluid mechanics. Krieger Publishing, Malabar, 457 pp

Wyngaard JC (1981) The effects of probe induced flow distortion on atmospheric-turbulence measurements. J Appl Meteorol 20(7):784–794